

Very Light Axigluons and the Top Asymmetry

Gordan Z. Krnjaic^{1,2}

1) *Theoretical Physics Department, Fermilab, Batavia, IL 60510, USA*

2) *Department of Physics and Astronomy, Johns Hopkins University, Baltimore, MD 21218, USA*

June 2, 2019

We show that very light (50 – 90 GeV) axigluons with flavor-universal couplings of order 0.4 may explain the anomalous top forward-backward asymmetry reported by both CDF and D0 collaborations. The model is naturally consistent with the observed $t\bar{t}$ invariant mass distribution and evades bounds from light Higgs searches, LEP event shapes, and measurements of the hadronic Z width. Very light axigluons can appear as resonances in multijet events, but searches require sensitivity to masses below current limits.

1 Introduction

The CDF and D0 collaborations have recently reported measurements of the forward-backward asymmetry (A_{FB}) in $t\bar{t}$ production with intriguing deviations from the standard model prediction. CDF’s result [1] in the lepton plus jets channel reports an inclusive parton level asymmetry

$$A_{FB}(\text{CDF})_{\ell j} = (15.8 \pm 7.4)\% . \quad (1.1)$$

If their measurement in the dilepton channel [2] is combined with this result, the asymmetry becomes

$$A_{FB}(\text{CDF})_{\ell\ell+\ell j} = (20.9 \pm 6.6)\% , \quad (1.2)$$

and exceeds the standard model prediction $\simeq 5\%$ [3]-[5] by more than 2 standard deviations.

D0 performs a similar search [6] in the lepton plus jets channel and reports an inclusive parton-level asymmetry

$$A_{FB}(\text{D0})_{\ell j} = (19.6 \pm 6.5)\% , \quad (1.3)$$

which is also more than 2σ above the SM result. Taken together, these consistent deviations may be evidence for new physics in top quark production.

While all the inclusive measurements are consistent with each other, CDF’s lepton plus jets search sees sharp mass dependence [1] in the binned result

$$\begin{aligned} A_{FB}(M_{t\bar{t}} < 450 \text{ GeV}) &= (-11.6 \pm 14.6)\% , \\ A_{FB}(M_{t\bar{t}} > 450 \text{ GeV}) &= (47.5 \pm 11.4)\% , \end{aligned}$$

where the high mass bin is 3.4σ above the SM prediction. Neither D0 nor the complimentary CDF dilepton search see the same effect; both find consistently positive $> 2\sigma$ deviations from the SM over the full $M_{t\bar{t}}$ range.

It has been observed that massive gluons with axial couplings can induce a large forward-backward asymmetry in $t\bar{t}$ production by interfering with standard model processes [7]-[12]. Motivated primarily by the mass dependent CDF result, these models predict asymmetries that rise uniformly with invariant mass and feature a sign flip near $M_{t\bar{t}} \approx 450$ GeV. Large (TeV scale) masses are typically required to satisfy dijet-resonance search bounds and suppress contributions to the $t\bar{t}$ invariant mass distribution. To produce an asymmetry with the observed sign, these models require flavor violation and are severely constrained [13] by limits on flavor changing neutral currents. For a comparison of heavy axigluons and other models that address the top asymmetry, see [14].

Relatively lighter axigluons (400 – 450 GeV) [15] can produce a large top asymmetry without flavor violation, but this mass scale is in tension with dijet resonance bounds and the differential $M_{t\bar{t}}$ distribution. Extra field content is generally required to broaden decay widths and avoid resonant enhancements to top quark observables.

In this paper we propose a *very light* (50 – 90

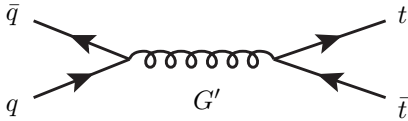


Figure 1: Axigluon contribution to $t\bar{t}$ pair production. Interference with the standard model gluon exchange diagram generates $\mathcal{A}_{int}^{G'}$.

GeV), weakly coupled axigluon to explain the top asymmetry. The model inherits many of the features heavier axigluons enjoy, but counterintuitively avoids their experimental constraints by being light: dijet resonance searches are insensitive to masses below a few hundred GeV, light particles below the $2m_t$ threshold do not produce bumps in the $t\bar{t}$ invariant mass distribution, and nonresonant production suppresses new physics contributions to the $t\bar{t}$ cross section, which start at fourth order in the axigluon coupling. We find that the strongest upper bounds in this range come from Tevatron searches for light Higgs bosons produced in association with an additional b -jet. The strongest lower bounds come from LEP measurements of the hadronic Z width.

In Section 2 we describe our model; in Section 3 we discuss the details of our numerical simulation; in Section 4 we address the experimental constraints; in Section 5 we compute the $t\bar{t}$ forward-backward asymmetry and compare theoretical predictions with production-level data; in Section 6 we make some concluding remarks.

2 Model Description

We give the axigluon (G') flavor universal couplings to SM quarks

$$\mathcal{L} \supset g' G'^a_{\mu} \bar{Q} T^a \gamma^{\mu} \gamma^5 Q , \quad (2.1)$$

where $g' \equiv \lambda g_s$ is the axigluon coupling constant, which we express in units of the strong coupling. This operator can arise from an extended $SU(3)_1 \times SU(3)_2$ color group that breaks down to the diagonal $SU(3)_c$ of QCD and gives rise to massive spin-1 color octets [16]-[19]. For an axigluon of mass $m_{G'}$ our effective model requires a UV completion at the scale $4\pi m_{G'}/g' = 1.7$ TeV and 850 GeV for $\lambda = 0.3$ and 0.6 respectively. In this paper, we will focus only on the low energy effective theory and leave UV model building for future work.

Without additional field content, all decays proceed through operator in Eq. (2.1), so axigluons can only decay to quark pairs and give rise to dijet and four jet events for single and pair production, respectively. Since we work in the regime where the axigluon is below the $t\bar{t}$ threshold, the total width is [20]

$$\Gamma_{G'} = \frac{n_f}{6} \alpha_s \lambda^2 m_{G'} , \quad (2.2)$$

where n_f is the number of active fermion flavors. For $m_{G'} = 80$ GeV and $\lambda = 0.4$, this width is $\Gamma_{G'} \simeq 1.1$ GeV.

The differential cross section for the process $q\bar{q} \rightarrow t\bar{t}$ in the CM frame is a sum of standard model, interference, and axigluon terms

$$\frac{d\hat{\sigma}(G')}{d\cos\theta} = \mathcal{A}_{SM} + \mathcal{A}_{int}^{G'} + \mathcal{A}_{axi}^{G'} , \quad (2.3)$$

where [21]

$$\mathcal{A}_{SM} = \frac{\pi \alpha_s^2 \beta}{9\hat{s}} \left(2 - \beta^2 + (\beta \cos\theta)^2 \right) , \quad (2.4)$$

$$\mathcal{A}_{int}^{G'} = \frac{4\pi \alpha_s^2 \lambda^2}{9} \frac{(\hat{s} - m_{G'}^2) \beta^2 \cos\theta}{(\hat{s} - m_{G'}^2)^2 + m_{G'}^2 \Gamma_{G'}^2} , \quad (2.5)$$

$$\mathcal{A}_{axi}^{G'} = \frac{\pi \alpha_s^2 \lambda^4}{9} \frac{\hat{s} \beta^3 (1 + \cos^2\theta)}{(\hat{s} - m_{G'}^2)^2 + m_{G'}^2 \Gamma_{G'}^2} . \quad (2.6)$$

Here $\beta \equiv \sqrt{1 - 4m_t^2/\hat{s}}$ is the top quark velocity and θ is the angle between the incoming quark and outgoing top in the CM frame. A forward-backward asymmetry can only arise from terms with odd powers of $\cos\theta$, so the effect is due entirely to interference. In the presence of both vector and axial-vector couplings, there is an additional small contribution to the asymmetry from the new-physics squared term.

Note that the asymmetry generating term $\mathcal{A}_{int}^{G'}$ is proportional to $(\hat{s} - m_{G'}^2)$. For heavier axigluons, this dependence gives rise to a negative asymmetry because the mass is typically larger than the partonic CM energy. To compensate, these models often require opposite sign couplings to the first and third generations. In our case, $m_{G'} < \hat{s}$ for on-shell $t\bar{t}$ production, so the asymmetry is always positive and flavor violation is unnecessary.

3 Simulation and Acceptances

In the lepton plus jets analysis, CDF unfolds raw data by deconvolving their detector simulation and jet algorithm to yield a partonic data set from events that survive cuts at the detector level. To compare our model predictions with this data, it is necessary to generate an event sample with partonic $t\bar{t}$ pairs in the final state. However, knowing the predicted cross section and experimental luminosity is not enough to properly normalize kinematic distributions from the partonic simulation; we must also know the detector level acceptances. We thus perform two simulations: one at the partonic level to make our plots and one at the detector level with CDF's cuts to compute the acceptances that normalize these distributions.

We simulate the partonic process $p\bar{p} \rightarrow t\bar{t}$ in MadGraph 5 [22] using a model file generated with FeynRules [23]. This file adds the operator in Eq. (2.1) to the full standard model Lagrangian so that the process in Figure 1 contributes to $t\bar{t}$ production and gives rise to interference with SM gluon-exchange.

For the acceptances, we also perform a more realistic simulation ($p\bar{p} \rightarrow t\bar{t} \rightarrow \ell\nu + 4j$) using PYTHIA [24] for the parton shower and PGS [25] for detector effects. To compare with CDF's lepton plus jets search, we impose the following cuts: at least four jets with $E_T > 20$ GeV and at least one b -tag; for non- b jets $|\eta_j| < 2$, for b -jets $|\eta_{bj}| < 1$; large missing energy $\cancel{E}_T > 20$ GeV; and exactly one electron or muon with $p_T^\ell > 20$ GeV and $|\eta_\ell| < 1$.

Note that there is some error introduced by this approximate method. A complete comparison with experimental data would not only run a full detector simulation (including PYTHIA and PGS), but also identify top quarks with a least-squares kinematic fitter and unfold the detector-level output using the CDF algorithm that reconstructs partonic events from raw data. Nonetheless, our approach accurately reproduces CDF's standard model expectation for the $t\bar{t}$ invariant mass distribution¹ so the error introduced by a constant acceptance function

¹ Although the forward-backward asymmetry arises only at loop level in the SM, its numerical value is tiny ($\sim 5\%$), so this tree level method also adequately reproduces the (largely symmetric) SM predictions for the $\Delta y = y_t - y_{\bar{t}}$ rapidity distributions in [1].

is likely to be small in our case as well. We leave the full unfolding for future work.

4 Experimental Constraints

Models that explain the top asymmetry must agree with the $t\bar{t}$ invariant mass distribution and total cross section, both of which are in good agreement with standard model predictions. Furthermore, any candidate model with an s -channel mediator must also satisfy bounds from dijet resonance searches from both Tevatron and LHC experiments. In our case, we must also contend with a variety older experiments that set lower bounds on new colored particles.

4.1 Top Quark Measurements

The $t\bar{t}$ cross section at the Tevatron has been measured to be $\sigma_{t\bar{t}}^{\text{exp.}} = 7.50 \pm 0.48$ pb [26], which agrees with the standard model prediction in perturbative QCD², $\sigma_{t\bar{t}}^{\text{sm}} \simeq (6.32 - 7.99)$ pb for $m_t = 172$ GeV [27]. The leading order result, $(\sigma_{t\bar{t}}^{\text{sm}})_{\text{LO}} \simeq 5.63$ pb, computed with MadGraph, implies a SM K -factor between 1.12 and 1.42.

Including an axigluon with $m_{G'} = 80$ GeV and $\lambda = 0.4$, gives a total LO cross section of $(\sigma_{t\bar{t}}^{\text{axi}})_{\text{LO}} = 6.08$ pb, which is only an 8% increase over the SM LO result. This minor enhancement is due entirely to $\mathcal{A}_{\text{axi}}^{G'}$ in Eq.(2.1), which is fourth order in the axigluon coupling; the interference term $\mathcal{A}_{\text{int}}^{G'}$ does not contribute to the total cross section. Although computing higher order corrections is beyond the scope of this work, the color structure of the axigluon exchange diagrams is identical to that of the relevant SM processes, so we expect higher order corrections to be of similar magnitude, though a more precise calculation is necessary to take into account the additional interference. As long as the K factor does not differ substantially from that of SM production, the total $t\bar{t}$ cross section stays in good agreement with experiment. For the remainder of this paper, we will assume the K factor to be 1.2, so our benchmark cross section becomes 7.3 pb.

For very light axigluons ($m_{G'} \ll 2m_t$), top pair production is nonresonant, so the invariant mass distribution also stays in good agreement with experi-

² For complementary calculations see [28, 29].

ment. In Figure 2 we show the simulated $M_{t\bar{t}}$ distribution (blue) plotted alongside the CDF data points and standard model background (purple) taken from the lepton plus jets search [1].

4.2 Dijet Resonance Searches

Quark coupled axigluons give rise to 2 and 4 jet events from single and pair production, respectively. Our mass range of interest (50 – 90 GeV) is safe from Tevatron [30, 31] and LHC [32, 33] dijet resonance searches, which do not set bounds on masses below 180 and 200 GeV, respectively. The UA2 experiment [34] is more sensitive to lower dijet masses, but axigluons with $m_{G'} < 130$ GeV are below their search threshold. A preliminary ATLAS analysis of multijet events [35] sets limits on color octet scalars with narrow widths, but does not bound masses below 100 GeV. With lower search thresholds, this model can be tested at both the Tevatron and LHC, however both signal and background are expected to be large at both colliders [36].

4.3 Light Higgs Searches

Tevatron searches that look for light Higgs bosons produced in association with b -jets ($p\bar{p} \rightarrow hb \rightarrow bbb$) are sensitive to axigluon decays into b -quarks. Since these searches require at least three b -tags to reduce the QCD multijet background, the bounds they impose on $\sigma(hb) \times \mathcal{Br}(h \rightarrow bb)$ also apply to the processes $p\bar{p} \rightarrow G'b \rightarrow bbb$ and $p\bar{p} \rightarrow G'bb \rightarrow bbbb$, the latter of which can also arise from pair produced axigluons. However, the CDF [37] and D0 [38] results only apply to masses above 90 GeV; light axigluons fall below the sensitivity threshold. To be conservative, we will only consider masses below 90 GeV where the $3b$ constraints do not apply.

The authors in [39] use Tevatron Higgs searches in the associated production channel, $p\bar{p} \rightarrow Wh \rightarrow (\ell\nu)(b\bar{b})$ to exclude axigluons with $\lambda = 1$ between 75 – 125 GeV assuming $\mathcal{Br}(G' \rightarrow b\bar{b}) = 1/5$. In our case with $\lambda = 0.4$, the Tevatron $q\bar{q} \rightarrow WG'$ cross section decreases by a factor of λ^2 , which reduces the constrained observable $\sigma \times \mathcal{Br}$ from ≈ 50 pb down to ≈ 5 pb for $m_{G'} = 50$ GeV. This falls safely below the quoted bound of $\lesssim 20$ pb, however, this number is based on analysis from an unpublished talk, so its status is not clear. Current Tevatron searches for

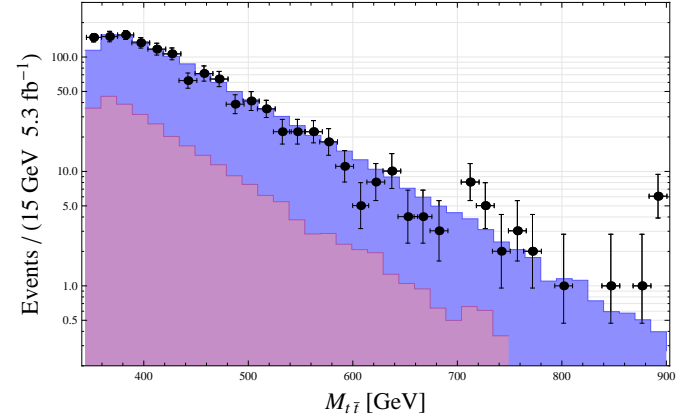


Figure 2: Tevatron invariant mass distribution for $t\bar{t}$ pairs (blue) including both axigluon and background contributions. Data points and standard model background (purple) are taken from CDF’s lepton plus jets search [1]. Here we use $\lambda = 0.4$ and $m_{G'} = 80$ GeV. After including a K -factor of 1.2, the top cross section is $\sigma_{t\bar{t}} = 7.3$ pb. Applying the CDF cuts (see Section 3) gives an acceptance of 2.6%.

the associated production of Higgs bosons are not sensitive to masses below 100 GeV [40, 41].

4.4 Event Shapes

Generic bounds on light colored particles can be extracted from the analysis of event shapes at LEP. Comparing this data with calculations in soft collinear effective theory (SCET) excludes color adjoint fermions below 51 GeV at 95% confidence [42]. However, this analysis assumes that the new field couples only to gluons, with no tree-level quark interactions. To apply this result to our case, the full analysis would have to be repeated with more general assumptions. Since such a reanalysis would likely set a comparable bound for our model, we will only consider masses above 51 GeV.

4.5 Running of α_s

Since axigluons couple to the strong sector, they give rise to loop diagrams that modify the QCD beta function above the scale $m_{G'}$. The standard model running between energy scales Q and μ is given by

$$\alpha_s(Q^2) = \frac{\alpha_s(\mu^2)}{1 + b \alpha_s(\mu^2) \log \left(\frac{Q^2}{\mu^2} \right)} , \quad (4.1)$$

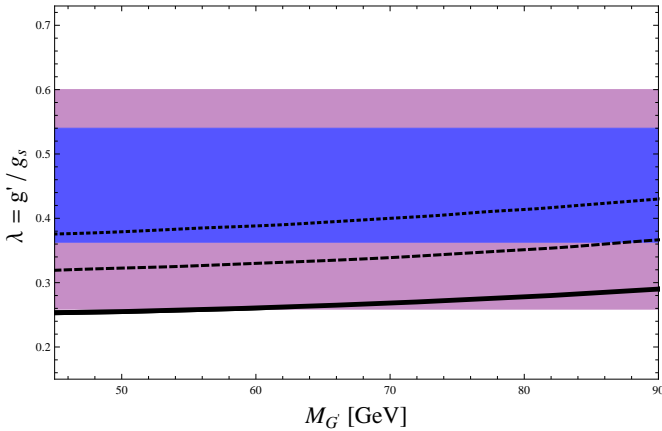


Figure 3: Allowed axigluon parameter space in the $(\lambda, m_{G'})$ plane plotted alongside bounds from $\Gamma(Z \rightarrow \text{hadrons})$ with different extractions of α_s . The blue and purple bands (color online) are regions favored by the combined CDF/D0 inclusive asymmetry measurements at 1σ and 2σ , respectively. The solid curve assumes the standard model extraction $\alpha_s(m_Z) = g_s^2/4\pi = 0.1184$ and marks the boundary where corrections to the hadronic Z width exceed the measured central value by 2σ . The dashed and dotted curves respectively assume 2.5% and 5% reductions to the SM value of $\alpha_s(m_Z)$. Reductions of this magnitude are typical of light axigluon contributions to the QCD beta function (for a discussion see Sections 4.6 and 4.5). The region above $m_{G'} > 90$ GeV is excluded by Tevatron 3b-searches. Since LEP event shapes rule out gluon-coupled adjoint fermions below 51 GeV, we conservatively expect a similar lower bound to apply in our case.

where, to leading order, $b = (33 - 2n_f)/12\pi$ and n_f is the number of active fermion flavors. Since axigluons have the same quantum numbers and self couplings as gluons, their principal effect on the running is to double the gluon contribution to the beta function above $m_{G'}$: $b \rightarrow (2 \times 33 - 2n_f)/12\pi$. This accelerates asymptotic freedom and yields smaller values of α_s near the weak scale.

While this adjustment naïvely jeopardizes the agreement between theory and experiment for the running, the experimental extraction of α_s depends entirely on the assumed validity of standard model QCD with no additional field content [43]. At each energy scale, an α_s -dependent observable is equated to the SM prediction and the resulting data point is

extracted implicitly. If light new states were present in the strong sector, this data would completely ignore their contributions, so the current agreement between theory and experiment does not constrain our model.

To roughly estimate the axigluon correction to $\alpha_s(m_Z)$, we use a well-measured value of α_s below $m_{G'}$ as an IR boundary condition and evolve it with the new beta function. This method is crude because even low-energy observables used to extract α_s depend somewhat on virtual axigluon processes, which are ignored in the extraction of reported measurements. Nonetheless, using the boundary condition $\alpha_s(14.9 \text{ GeV}) = 0.160$, [43] the weak-scale value becomes $\alpha_s(m_Z) = 0.105, 0.110$, and 0.115 for $m_{G'} = 50, 65$ and 80 GeV, respectively. Different IR boundary conditions give similar downward corrections of order a few percent relative to the SM extraction $\alpha_s(m_Z) = 0.1184$. Note that this result is independent of λ since axigluons couple to gluons with QCD strength.

This model also predicts a kink in the running of α_s near $m_{G'}$. Our mass range of interest ($50 - 90$ GeV), however, overlaps with a region where data points are sparsely distributed with relatively large error bars (see Figure 6 in [43]) compared to the data set as a whole. Kinks in the slope of α_s would, therefore, be unlikely to stand out in the data. Nonetheless, a model-dependent extraction of α_s is necessary to evaluate the possibility of kinks or overall data shifts due to new physics contributions.

4.6 Hadronic Z Width

The strongest lower bound on $m_{G'}$ comes from virtual and three-body corrections to the hadronic Z width. Axigluons that couple to quarks with QCD strength ($\lambda = 1$) enhance this width by a factor of

$$1 + \frac{\alpha_s}{\pi} f(m_Z/m_{G'}) + \mathcal{O}(\alpha_s^2) , \quad (4.2)$$

where f is a function derived in [44, 45]. The LEP measurement of $\Gamma(Z \rightarrow \text{hadrons})$ and the extracted value of $\alpha_s(m_Z)$ constrain the size of $f(m_Z/m_{G'})$ and severely restrict axigluon masses: $m_{G'} > 570$ (365) GeV for $\lambda = 1$ at the 65% (95%) confidence level [39].

However, f is highly nonlinear, so the mass constraint is *extremely* sensitive to the axigluon coupling. In our scenario, the constraint on f applies

to the combination $\lambda^2 f$, which dramatically weakens the lower bound on $m_{G'}$. Furthermore, following the discussion in Section 4.5, light axigluon ($m_{G'} < m_Z$) contributions to the QCD beta function generically decrease the value of $\alpha_s(m_Z)$ at the percent level. Since this is used to compute the SM prediction for $\Gamma(Z \rightarrow \text{hadrons})$, a smaller value opens up more allowed parameter space for new physics; the positive axigluon contribution to the width compensates for a slightly smaller SM result which is reduced by the new value of α_s .

In Figure 3 we plot 2σ exclusion bounds from the hadronic Z width on the $(\lambda, m_{G'})$ plane alongside the regions favored by combined CDF and D0 A_{FB} measurements (discussed in Section 5). The solid black curve uses the standard model extraction $\alpha_s(m_Z) = 0.1184 \pm 0.0007$ [43] and the measured $\Gamma(Z \rightarrow \text{hadrons}) = 1.744 \pm 0.002$ GeV [46] to identify parameters for which the theoretical prediction exceeds the measured central value by 2σ . Also plotted are the 2σ bounds assuming 2.5 % (dashed) and 5% (dotted) reductions in $\alpha_s(m_Z)$ due to the modified running that includes axigluon contributions. These curves show how sensitive the bound is to modifications in λ and $\alpha_s(m_Z)$. Since we generically expect light axigluons to reduce the value of $\alpha_s(m_Z)$ by a few percent relative to the SM extraction, the dashed and dotted curves are more faithful to the underlying physics. Given the sensitivity of the bound, a proper extraction of α_s involving axigluon processes is necessary to accurately constrain the parameter space; the limits in Figure 3 serve merely to illustrate the impact on the allowed region.

4.7 Bounds from $\sigma(e^+e^- \rightarrow \text{hadrons})$

The authors in [44] calculate ³ axigluon corrections to the ratio

$$R(s) \equiv \frac{\sigma(e^+e^- \rightarrow \text{hadrons})}{e^4/12\pi s} \quad (4.3)$$

at the scale $\sqrt{s} = 34$ GeV and thereby exclude masses below 50 GeV at 95% confidence assuming $\lambda = 1$. As with the hadronic Z width, the corrections for this process are proportional to the factor

³Note that [44] corrects some minor, yet consequential errors from an earlier paper [45] that placed a far stronger lower bound on the mass.

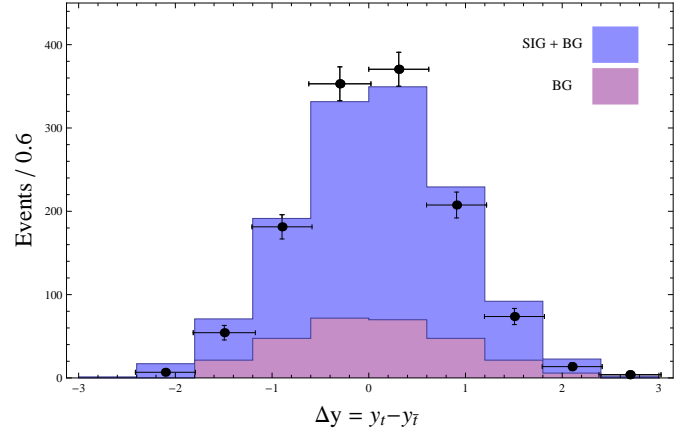


Figure 4: Inclusive top anti-top rapidity difference distribution plotted against unfolded CDF data. Here we use the same model parameters as in Fig. 2. The blue histograms include both signal and standard model background. Both data and background (purple) are taken from [1]. This plot omits the small, loop level asymmetry generated by SM processes.

in Eq. (4.2) with the replacement $\alpha_s \rightarrow \lambda^2 \alpha_s$, so the discussion in Section 4.6 applies to this bound as well. Since $\Gamma(Z \rightarrow \text{hadrons})$ is extracted from R data at the Z pole, the allowed parameter space in Figure 3 is automatically consistent with bounds from R near $\sqrt{s} = m_Z$. For smaller energies in our range of interest, $\sqrt{s} \in 50 - 90$ GeV, the uncertainties on the R data are larger than those at the Z pole [46], so the bound is weaker.

5 Forward Backward Asymmetry

The forward-backward asymmetry can be written

$$A_{FB} \equiv \frac{N(\Delta y > 0) - N(\Delta y < 0)}{N(\Delta y > 0) + N(\Delta y < 0)} , \quad (5.1)$$

where $\Delta y \equiv y_t - y_{t̄}$ is the rapidity difference between the top and anti-top quarks.

In Figure 3 we show the favored parameter space in the $(\lambda, m_{G'})$ plane. The blue (purple) band represents the region of 1σ (2σ) agreement with the combined CDF, Eq. (1.2), and D0, Eq.(1.3) inclusive measurements. For typical points in these regions, the model predicts a positive asymmetry of order 20%.

In Figure 4 we show the inclusive $t\bar{t}$ rapidity-difference distribution plotted against the CDF data.

The signal simulation is identical to that used to generate Figure 2 with $m_{G'} = 80$ GeV and $\lambda = 0.4$. After applying the cuts described in Section 3, the acceptance is 2.6%. This plot only depicts the effects of tree-level processes; the histograms do not include the small asymmetry induced by standard model processes. However, the numerical results in Fig. 3 include the full asymmetry with both SM and new physics contributions.

Although our simulation gives an acceptable fit to the rapidity data, some of the bins are more than 1σ away from data points. We, however, do not expect perfect agreement at this level of analysis. The distribution in Figure 4 is a rough approximation of the full theory prediction which requires both a full CDF detector simulation and the subsequent unfolding for a proper comparison with data.

In Figure 5 we show the theory prediction for the mass dependent asymmetry $A_{FB}(M_{t\bar{t}})$ plotted alongside the unfolded CDF data. Like other light s channel mediators, light axigluons predict a positive asymmetry throughout the whole range of invariant masses. While the agreement at low invariant mass is not ideal, neither D0 nor the CDF dilepton measurement observe strong mass dependence, so the significance of the mass-dependent data is not clear.

Note that in Figures 2, 4 and 5 we only compare the model to CDF results because their published distributions feature production-level data, which allow for a direct comparison with parton level simulations. Comparison with D0's distributions requires a detailed understanding of their detector simulation, which is beyond the scope of this work. Our conclusions have emphasized inclusive results from both collaborations since these are in better agreement with each other than the more controversial mass-dependent data.

6 Conclusions

We have shown that a light axigluon with flavor universal couplings can generate a large, positive $t\bar{t}$ asymmetry and naturally agrees with measurements of $d\sigma/dM_{t\bar{t}}$. The model has viable parameter consistent with light Higgs bounds, dijet resonance searches and measurements of the hadronic Z width.

For masses between 50 – 90 GeV and quark couplings in the range 0.3 – 0.6, the theoretical predic-

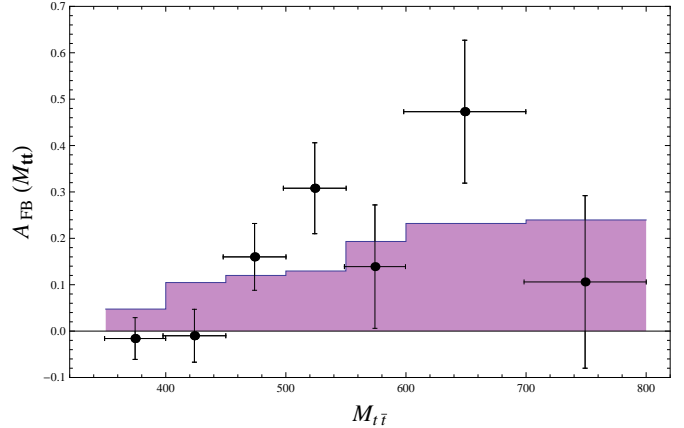


Figure 5: Theory prediction for the mass dependent $t\bar{t}$ asymmetry (purple histograms) plotted against the binned, unfolded CDF data in the lepton plus jets channel [1]. Here we use the same model parameters as in Fig. 2. For comparison with CDF, the bin sizes are 50 GeV for $M_{t\bar{t}} < 600$ GeV and 100 GeV for larger invariant masses. Since the interference term in the differential cross section, Eq. (2.5), is proportional to $(\hat{s} - m_{G'}^2)$, the asymmetry is always positive for on-shell $t\bar{t}$ production. This is a generic feature of light axigluon models.

tion for the parton-level top asymmetry is in good agreement with both CDF and D0 results. The asymmetry is proportional to $(\hat{s} - m_{G'}^2)$, so the sign of A_{FB} is always positive for on-shell top production with $\sqrt{s} > 2m_t$, which agrees with the inclusive results from both collaborations.

In the presence of a light axigluon, both the predicted and observed values of $\alpha_s(\sqrt{s})$ are modified at the percent level. A reanalysis of $\alpha_s(\sqrt{s})$ measurements should reveal downward shifts in the data; the revised beta function accelerates the running of α_s to maintain agreement between theory and experiment. The downward shift in α_s also decreases the SM predictions for $\Gamma(Z \rightarrow \text{hadrons})$ and $\sigma(e^+e^- \rightarrow \text{hadrons})$, which opens up parameter space for larger new physics contributions to both observables. This expands the allowed region in the $(\lambda, m_{G'})$ plane to include parameters that are simultaneously consistent with LEP observables and explain the top forward-backward asymmetry.

If very light axigluons explain the top forward-backward asymmetry, both the Tevatron and LHC should observe resonances in 2 and 4 jet events from single and pair production. Although the QCD back-

ground in our mass range is formidable, in principle it is possible to observe dijet resonances from both samples and reconstruct the axigluon mass.

Acknowledgments: We thank Bogdan Dobrescu, Patrick Fox, Graham Kribs, Roni Harnik, and David E. Kaplan for helpful discussions. GZK is supported by a Fermilab Fellowship in Theoretical Physics. Fermilab is operated by Fermi Research Alliance, LLC, under Contract DE-AC02-07-CH11359 with the US Department of Energy.

References

- [1] T. Aaltonen *et al.* [CDF Collaboration], Phys. Rev. **D83**, 112003 (2011), [[arXiv:1101.0034](https://arxiv.org/abs/1101.0034)].
- [2] CDF Public Note, [10436].
- [3] J. H. Kuhn and G. Rodrigo, Phys. Rev. D **59**, 054017 (1999), [[arXiv:9807420](https://arxiv.org/abs/9807420)].
- [4] V. Ahrens, A. Ferroglio, M. Neubert, B. D. Pecjak and L. L. Yang, [[arXiv:1106.6051](https://arxiv.org/abs/1106.6051)].
- [5] M. T. Bowen, S. D. Ellis, D. Rainwater, Phys. Rev. **D73**, 014008 (2006), [[arXiv:0509267](https://arxiv.org/abs/0509267)].
- [6] D0 Collaboration, [[arXiv:1107.4995](https://arxiv.org/abs/1107.4995)].
- [7] O. Antunano, J. H. Kuhn and G. Rodrigo, Phys. Rev. D **77**, 014003 (2008), [[arXiv:0709.1652](https://arxiv.org/abs/0709.1652)].
- [8] P. H. Frampton, J. Shu and K. Wang, Phys. Lett. B **683**, 294 (2010), [[arXiv:0911.2955](https://arxiv.org/abs/0911.2955)].
- [9] M. Bauer, F. Goertz, U. Haisch, T. Pfoh, S. Westhoff, JHEP **1011**, 039 (2010), [[arXiv:1008.0742](https://arxiv.org/abs/1008.0742)].
- [10] Y. Bai, J. L. Hewett, J. Kaplan and T. G. Rizzo, JHEP **1103**, 003 (2011), [[arXiv:1101.5203](https://arxiv.org/abs/1101.5203)].
- [11] A. R. Zerwekh, [[arXiv:1103.0956](https://arxiv.org/abs/1103.0956)].
- [12] E. Alvarez, L. Da Rold, J. I. S. Vietto and A. Szynkman, [[arXiv:1107.1473](https://arxiv.org/abs/1107.1473)].
- [13] R. S. Chivukula, E. H. Simmons and C. P. Yuan, Phys. Rev. D **82**, 094009 (2010), [[arXiv:1007.0260](https://arxiv.org/abs/1007.0260)].
- [14] M. I. Gresham, I. -W. Kim, K. M. Zurek, Phys. Rev. **D83**, 114027 (2011), [[arXiv:1103.3501](https://arxiv.org/abs/1103.3501)].
- [15] G. Tavares, M. Schmaltz [[arXiv:1107.0978](https://arxiv.org/abs/1107.0978)].
- [16] L. J. Hall and A. E. Nelson, Phys. Lett. B **153**, 430 (1985), [Journal Server].
- [17] P. H. Frampton, S. L. Glashow, Phys. Lett. **B190**, 157 (1987). [Journal Server].
- [18] C. T. Hill, S. J. Parke, Phys. Rev. **D49**, 4454-4462 (1994), [[arXiv:hep-ph/9312324](https://arxiv.org/abs/hep-ph/9312324)].
- [19] C. T. Hill, Phys. Lett. **B266**, 419-424 (1991), [Journal Server].
- [20] P. Ferrario and G. Rodrigo, Phys. Rev. D **78**, 094018 (2008), [[arXiv:0809.3354](https://arxiv.org/abs/0809.3354)].
- [21] Q. H. Cao, D. McKeen, J. L. Rosner, G. Shaughnessy, C. E. M. Wagner, Phys. Rev. **D81**, 114004 (2010), [[arXiv:1003.3461](https://arxiv.org/abs/1003.3461)].
- [22] J. Alwall, M. Herquet, F. Maltoni, O. MatteLaer, T. Stelzer, [[arXiv:1106.0522](https://arxiv.org/abs/1106.0522)].
- [23] N. D. Christensen, C. Duhr, Comput. Phys. Commun. **180**, 1614-1641 (2009), [[arXiv:0806.4194](https://arxiv.org/abs/0806.4194)].
- [24] T. Sjostrand, S. Mrenna and P. Skands, JHEP **0605**, 026 (2006), [[arXiv:0603175](https://arxiv.org/abs/0603175)].
- [25] J. S. Conway, Pretty Good Simulation (PGS).
- [26] CDF Public Note, [9913].
- [27] S. Moch, P. Uwer, Phys. Rev. **D78**, 034003 (2008), [[arXiv:0804.1476](https://arxiv.org/abs/0804.1476)].
- [28] N. Kidonakis and R. Vogt, Phys. Rev. D **78**, 074005 (2008), [[arXiv:0805.3844](https://arxiv.org/abs/0805.3844)].
- [29] M. Cacciari, S. Frixione, M. L. Mangano, P. Nason and G. Ridolfi, JHEP **0809** (2008) 127, [[arXiv:0804.2800](https://arxiv.org/abs/0804.2800)].
- [30] T. Aaltonen *et al.* [CDF Collaboration], Phys. Rev. D **79**, 112002 (2009), [[arXiv:0812.4036](https://arxiv.org/abs/0812.4036)].
- [31] V. M. Abazov *et al.* [D0 Collaboration], Phys. Rev. D **69**, 111101 (2004), [[arXiv:0308033](https://arxiv.org/abs/0308033)].
- [32] G. Aad *et al.* [ATLAS Collaboration], New J. Phys. **13**, 053044 (2011), [[arXiv:1103.3864](https://arxiv.org/abs/1103.3864)].

- [33] V. Khachatryan *et al.* [CMS Collaboration], Phys. Rev. Lett. **105**, 211801 (2010), [[arXiv:1010.0203](https://arxiv.org/abs/1010.0203)].
- [34] J. Alitti *et al.* , Nucl. Phys. B **400**, 3 (1993), [UA2 Collaboration].
- [35] J. Zhu [ATLAS Collaboration], [SUSY '11 Plenary Talk].
- [36] B. A. Dobrescu, K. Kong, R. Mahbubani, JHEP **0707**, 006 (2007), [[arxiv:0703231](https://arxiv.org/abs/0703231)].
- [37] T. Aaltonen *et al.* [CDF Collaboration], [[arXiv:1106.4782](https://arxiv.org/abs/1106.4782)].
- [38] V. M. Abazov *et al.* [D0 Collaboration], Phys. Rev. Lett. **101**, 221802 (2008), [[arXiv:0805.3556](https://arxiv.org/abs/0805.3556)].
- [39] M. A. Doncheski, R. W. Robinett, Phys. Rev. **D58**, 097702 (1998), [Journal Server].
- [40] CDF Collaboration, [W+ Higgs Limits].
- [41] D0 Collaboration, [W+ Higgs Limits].
- [42] D. E. Kaplan, M. D. Schwartz, Phys. Rev. Lett. **101**, 022002 (2008), [[arXiv:0804.2477](https://arxiv.org/abs/0804.2477)].
- [43] S. Bethke, Eur. Phys. J. **C64**, 689-703 (2009), [[arXiv:0908.1135](https://arxiv.org/abs/0908.1135)].
- [44] F. Cuypers, A. F. Falk, P. H. Frampton, Phys. Lett. **B259**, 173-174 (1991), [Journal Server].
- [45] F. Cuypers, P. H. Frampton, Phys. Rev. Lett. **63**, 125-127 (1989), [Journal Server].
- [46] K. Nakamura *et al.* [Particle Data Group Collaboration], J. Phys. G **G37**, 075021 (2010), [PDG Online].